Thermodynamic anomalies and three distinct liquid-liquid transitions in warm dense liquid hydrogen

Hua Y. Geng,[1,2,*] Q. Wu,[1] Miriam Marqués,[3] and Graeme J. Ackland [3]

[1]*National Key Laboratory of Shock Wave and Detonation Physics, Institute of Fluid Physics, CAEP, P.O. Box 919-102, Mianyang, Sichuan 621900, People's Republic of China*

[2]*Center for Applied Physics and Technology, HEDPS, and College of Engineering, Peking University, Beijing 100871, China*

[3]*CSEC, SUPA, School of Physics and Astronomy, The University of Edinburgh, Edinburgh EH9 3JZ, United Kingdom*

The properties of hydrogen at high pressure have wide implications in astrophysics and high-pressure physics. Its phase change in liquid is variously described as metallization, H_2 dissociation, density discontinuity, or plasma phase transition. It has been tacitly assumed that these phenomena coincide at a first-order liquid-liquid transition. In this work, the relevant pressure-temperature conditions are thoroughly explored with first-principles molecular dynamics. We show that there is a large dependency on the exchange-correlation functional and significant finite-size effects. We use hysteresis in a number of measurable quantities to demonstrate a first-order transition up to a critical point, above which molecular and atomic liquids are indistinguishable. At higher temperature beyond the critical point, H_2 dissociation becomes a smooth crossover in the supercritical region that can be modeled by a pseudotransition, where the $H_2 \leftrightarrow 2H$ transformation is localized and does not cause a density discontinuity at metallization. Thermodynamic anomalies and the counterintuitive transport behavior of protons are also discovered even far beyond the critical point, making this dissociative transition highly relevant to the interior dynamics of Jovian planets. Below the critical point, simulation also reveals a dynamic $H_2 \rightarrow 2H$ chemical equilibrium with rapid interconversion, showing that H_2 and H are miscible. The predicted critical temperature lies well below the ionization temperature. Our calculations unequivocally demonstrate that there are three distinct regimes in the liquid-liquid transition of warm dense hydrogen: A first-order thermodynamic transition with density discontinuity and metallization in the subcritical region, a pseudotransition crossover in the supercritical region with metallization without density discontinuity, and finally a plasma transition characterized by the ionization process at very high temperatures. This feature and the induced anomalies originate in the dissociative transition nature that has a negative slope in the phase boundary, which is not unique to hydrogen but is a general characteristic shared by most dense molecular liquids. The revealed multifaceted nature of this dissociative transition could have an impact on the modeling of gas planets, as well as the design of H-rich compounds.

I. INTRODUCTION

Hydrogen is a simple element, but it exhibits complex behavior at high pressures. Rich physics and chemistry have been discovered, and they are still being predicted in both pure hydrogen [1–3] and hydrogen-rich compounds [4–7]. Dense solid hydrogen shows an unexpectedly complicated phase diagram [8–15] with an anomalous melting curve maximum and minimum [3,16–21], embodying solid states based around free rotating molecules (phase I), broken symmetry due to quadrupole interactions (phase II), packing of weakly bonded molecules (phase III), and proposed "mixed" state (phases IV and V). The latter two phases have alternating layers of rotating molecules similar to phase I, and weak molecules akin to phase III [1,13,15]. Other phases under extreme compression include the recently claimed (and still controversial)

molecular conductor or atomic metal [12,22,23], the predicted mobile solid state [2,21], and superconducting superfluid quantum liquid [24–26]. This wide range of behavior highlights the significance of dense hydrogen as an *archetype* of a many-body quantum system [23,24,27].

At sufficiently high pressure, liquid hydrogen becomes metallic. This is associated with the electronic transition from molecular H_2 to atomic H [28–30]. Historically, H_2 dissociation (i.e., $H_2 \rightarrow 2H$) at high pressure was first proposed as a process that coincides with the *ionization* in which electrons leave the H_2 successively, namely $H_2 \rightarrow H_2^+ + e \rightarrow 2H^+ + 2e$ [31]. The resultant state would be a plasma; therefore, the corresponding transition is termed a plasma phase transition (PPT) [32,33]. Recent high-pressure investigations, however, suggested that the molecular dissociation temperature should be related to *covalent bond-breaking* energies, rather than full ionization [27,34–38]. All experimental and simulation evidence indicates that this liquid-liquid transition (LLT) and metallization can occur at temperatures well below the *ionization energy*. In other words, dissociation of liquid hydrogen

at low temperature is intrinsically a unique phase transition *different* from the PPT.

The nature of this low-temperature transition has been under debate for a long time [39–43,51]. Recent calculations based on density functional theory (DFT) and quantum Monte Carlo (QMC) suggested that it should be a *first-order* transition terminated at a *critical point* (CP), and be coincident with the metallization at low temperatures [35,44–46]. However, like ionization, a localized and uncorrelated thermally activated process of bond-breaking should not yield a first-order transition involving a *collective* change; it must couple to other variables to induce the required large-scale correlations. Specifically, quantitative disagreement about the transition line remains. The critical temperature early estimated using DFT [via kinks in the equation of state (EOS)] gave $T_c \approx$ 2000 K [44,45]. A recent coupled electron-ion Monte Carlo (CEIMC) estimation is between 1000 and 1500 K [35]. By checking the variation of proton-proton radial distribution functions (RDFs) calculated with DFT, Norman *et al.* claimed an unusually high $T_c \geqslant 4000$ K [47]. A recent but not well-converged DFT simulation also reported a similar T_c [48]. The latest variational Monte Carlo–molecular dynamics (VMC-MD) estimation of T_c was between 3000 and 6000 K, also identified via small kinks in the EOS [46].

Another open question is whether dissociation involves H_3^+ cations [46,47,49]. This is important not only because they were used as a diagnostic to determine the transformation T_c [46,47], but also because in design of H-rich superconductors it is a prerequisite to form large H-clusters or clathrate structures [4–6] that can be viewed as an *intermediate step* in hydrogen dissociation where the electron-phonon coupling is being maximized.

Finally, the atomic and molecular H miscibility and transport properties near or below the critical point are still unknown, and they require larger supercells than are typically used to correctly describe liquid structure [50]. They are of great significance for modeling the convective flow crossing the H_2/H layer in giant gas planets [31,34]. Therefore, despite all these previous works, a central question remains: are all relevant physical quantities discontinuous at a *single*, *first-order*, LLT in warm dense liquid hydrogen?

By using well-constrained and converged first-principles simulations, we addressed these important issues. The pressure of the LLT turns out to be extremely sensitive to the choice of exchange-correlation functional, while the critical temperature T_c of LLT is better characterized and found to lie between 1000 and 1500 K. This supports the latest National Ignition Facility (NIF) experimental assessment [51] and the CEIMC result [35], but it contradicts the previous DFT [47] and VMC-MD [46] assertion. In addition, H_3 clusters can be frequently identified by the proximity of three atoms, but the lifetime is shown to be too short to produce any spectroscopic signature or for H_3 to be sensibly regarded as a chemical species.

For a first-order transition with a discontinuous density and electric conductivity at the LLT, one also expects a distinct two-phase coexistence interface. Nonetheless, we find that such phase separation is *impossible* because of the rapid H_2-2H interconversion. More importantly for planetary

dynamics, we demonstrate a counterintuitive increase in the proton self-diffusivity with pressure.

The paper is organized as follows. In Sec. II we present the methodology and computational details. The main results and discussion are given in Sec. III, which covers the topics of miscibility of H_2/H, a careful estimate of the critical temperature at ~1250 K at the DFT level, the low probability of H_3 clusters and their short lifetime, anomalous thermodynamics and proton transportation in the vicinity of the dissociative transition, a pseudotransition model for this transition beyond the critical point (i.e., in the supercritical region), and the three distinct LLT regimes. Finally, in Sec. IV, further discussion and the potential impact on the interior dynamics of gas planets are presented, with Sec. V providing a summary of the main results.

II. METHODOLOGY AND COMPUTATIONAL DETAILS

The first-principles calculations were carried out using DFT and a projector augmented-wave pseudopotential for the ion-electron interaction, and with two different exchange-correlation functionals for the electron subsystem: the generalized gradient approximation of Perdew, Burke, and Ernzerhof (PBE), and the van der Waals functional of vdW-DF (specifically, revPBE-vdW) [52,53], as implemented in VASP, to constrain the results. It is well recognized that PBE is deficient in describing H_2 metallization pressure [54,55]. But it can be expected that the true physics in dense hydrogen near dissociation is bracketed by PBE and vdW-DF, with the former underestimating the dissociation pressure whereas the latter overstabilizes the H_2 molecule [56,57], as both the recent accurate CEIMC calculations [35] and dynamic compression experiments [27] suggested. At a fixed density near the dissociation, it was estimated that PBE (vdW-DF) underestimated (overestimated) the pressure by about 10–20 GPa in hydrogen. These two functionals are therefore employed simultaneously in this work to get a reliable assessment of the unknown systematic error in DFT.

In *ab initio* molecular dynamics (AIMD) simulations, supercells containing up to 3456 hydrogen atoms with periodic boundary conditions were employed. The radial distribution function (RDF) shows four well-defined molecular shells that are captured in the 500-atom supercells that form the basis of our work, but they would be destroyed by periodic boundary condition artifacts in simulations with smaller system sizes. The Baldereschi mean point is utilized for k-point sampling, which has been carefully checked for liquid hydrogen and gives an accuracy equivalent to a $4 \times 4 \times 4$ mesh [39,45]. This setting is necessary to eliminate the possible spurious structures in MD generated by single Γ-point sampling [58,59]. By contrast, Ref. [48] employed a much smaller system with 64 atoms and a $3 \times 3 \times 3$ k-point mesh, which is obviously not well converged. The energy cutoff for the plane-wave basis set is 700 eV. The canonical ensemble (*NVT*) is used, with a time step of 0.5 fs. The temperature is controlled by a Nose-Hoover thermostat, and the conditions of thermodynamic equilibration and ergodicity are carefully checked. We find that the liquids equilibrate much faster than solids, so after equilibrating for 1 ps, further AIMD simulations are then carried out for 1.5 ps to gather ensemble-averaged statistics.
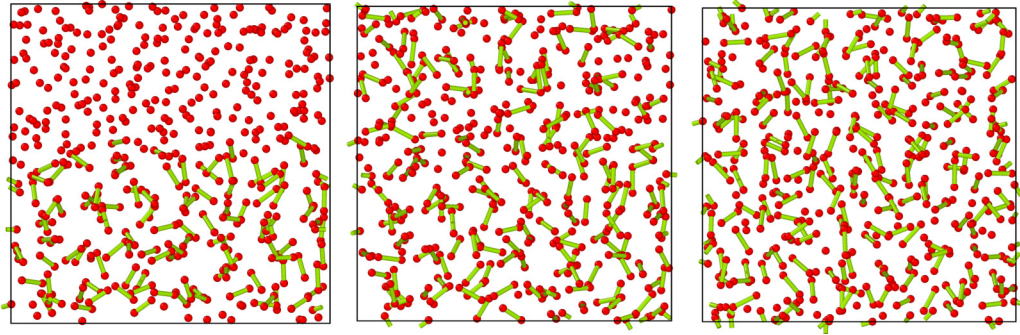
FIG. 1. Mixing of atomic H and molecular H_2 within the dissociation region around 125 GPa and 1500 K, calculated by AIMD with the PBE functional. Left panel: initial two-phase coexistence with a clear interface; middle panel: after 5 fs equilibrating, new bonds have formed in the upper region and bonds have broken in the lower region; right panel: after 950 fs equilibrating. The bond-length cutoff criterion for drawing green lines is set as 0.9 Å.

This enabled us to thoroughly explore finer *P-T* space, up to 500 GPa and from 500 to 3000 K. To check the sampling quality, some simulations were performed that were longer than 6 ps: these show smaller statistical fluctuations, but no different behaviors. The calculated PBE dissociation curve is in good agreement with previous estimates [27,44,45], which serves as direct validation of our method for the following calculations.

III. RESULTS AND DISCUSSION

A. H_2/H interface and miscibility

A discontinuous first-order LLT [35,44,45] implies that the material is expected to have a two-phase coexistence. Nonetheless, it is worth pointing out that two-phase coexistence does not necessarily guarantee a distinguishable two-phase *interface* in real space (i.e., the occurrence of phase separation). The latter appears only when the order parameters are quantities well-defined in real space, and the new phase *nucleates and grows* from a single embryo (or just a few). Otherwise, if there are infinite embryos, the transition might manifest as being homogeneous rather than heterogeneous. The LLT in hydrogen is further complicated because H_2 and H are distinct chemical species, and the reaction between these must be in chemical equilibrium. If this reaction occurs much faster than phase separation, it will appear as miscibility.

To investigate the H_2/H miscibility, we carried out AIMD simulations in the atomic-molecular hydrogen coexistence region, using two-phase coexistence as the initial condition. This is a standard method to determine the first-order transition boundary, such as melting [60,61]: the thermodynamically stable phase grows at the expense at the metastable one. As shown in Fig. 1, we find that the $H_2 \leftrightarrow 2H$ reaction is very fast, and the initial H_2/H interface disappears at the femtosecond scale, far more quickly than the boundary could move even at the speed of sound. There is no growth, movement, or evolution of the interface boundary in AIMD simulations. Instead, it is the formation of atomic H *inside* the H_2 domain and vice versa that causes this LLT [50]. This *reversible* chemical reaction proceeds much faster than the nucleation and growth process could. It also suggests that under this condition, the H_2 dissociation is mainly a *local* process in which the breaking or forming of individual H_2

dimers is insensitive to the local atomic environmental details. The same phenomena are also observed at 1000 K on the dissociation boundary, well below the previously estimated critical temperature [50].

This behavior is quite counterintuitive for a typical first-order transition, but it can be understood in terms of the unique thermodynamics of dense liquid hydrogen. Usually, a first-order phase transformation implies the existence of a density region, in which the total free energy is minimized by phase separation via binodal decomposition. If the density difference is a proper order parameter such as in the case of a liquid-vapor transition [Fig. 2(a)], it establishes an interface when the phase boundary is robust against thermal
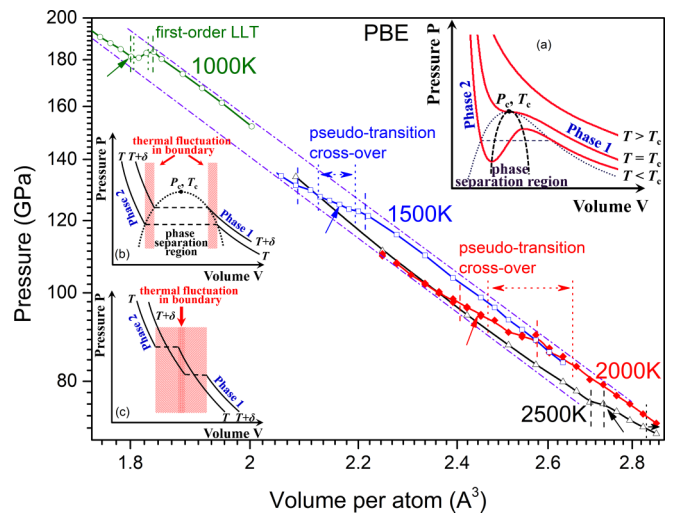

FIG. 2. Isothermal pressure-volume curves of warm dense liquid hydrogen across the dissociation region calculated with the PBE functional. A first-order LLT with distinct hysteresis is obtained at only low temperatures. The dash-dotted long lines are guides to the eye. Inset: (a) typical isotherms in the vicinity of the critical point for a normal first-order transition, below which there is a well-defined phase-separation region that gives rise to a two-phase coexistence interface; (b) variation in the phase boundary driven by thermal fluctuations of case (a); (c) schematic of isotherms for H_2 dissociation, in which the boundary variation induced by thermal fluctuations could eliminate the prohibited region completely (i.e., overlapping of the shaded regions).

disturbance [Fig. 2(b)]. Nonetheless, the snapshots of Fig. 1 and the calculated isotherms in the main panel of Fig. 2 show that the LLT of hydrogen clearly *does not* belong to this case. The isotherms belong to a type of Fig. 2(c) rather than Fig. 2(b). The real-space boundary of this type of transition (i.e., a two-phase interface) is *volatile* if subjected to thermal perturbations: it does not favor a phase separation in the pressure-density space, due to an intrinsic nature that originated in the negative slope of the phase boundary on the *P-T* space.

This unusual behavior can be understood further by regarding the molecular and atomic hydrogen as two different chemical species (i.e., viewing the transition as a chemical reaction). In this sense, the dissociative transition more or less relates to the concept of a "noncongruent" phase transition [62]. In the conventional phase-separation region, they would have the same free energy and can interconvert without any free-energy penalty. However, the molecular phase can lower its free energy still further through the increased entropy of mixing of H and H_2 after partial dissociation into atoms, and vice versa in the atomic phase. The equilibrium state is the same in both cases, i.e., the miscibility gap is wiped out, as shown by the hatched areas in Fig. 2(c). In a macroscopic picture for this kind of *abnormal* first-order LLT, the interfacial H_2/H free energy is negative, so the two-phase interface is volatile, and forming additional interfaces is favored. In terms of nucleation and growth, it means that the critical nucleus is infinitely small, so H_2 dissociation proceeds spontaneously and homogeneously with infinite micro-embryos, and it does not sustain a distinct and stable two-phase coexistence interface. This interesting scenario is further corroborated by the partial negative correlations in the bond length of the nearest-neighboring H_2 dimer along the dissociation [50], which also support H_2/H miscibility even below the critical point (i.e., in the subcritical region). It should be stressed that our calculations strongly support the idea that as a one-component system, hydrogen is realized as a "molecular" or "atomic" state depending on the *P-T* conditions, and in the transition region, hydrogen "molecules" are transient bound states or short-lived correlations, as their lifetime shown in [50] reveals.

The abnormality in H_2 dissociation also affects the thermodynamics in the vicinity of the dissociation region even *far beyond* the critical point where a conventional supercritical fluid should already become normal. For the isotherm calculations shown in Fig. 2, we find that both the thermal expansion coefficient and the pressure coefficient display a pronounced abnormal dip, reaching a negative value of about -6×10^{-5} K^{-1} and -1.2×10^{-4} K^{-1} at 2000 K, respectively, as shown in Fig. 3. By contrast, the compressibility has a peak in the dissociation region, which can be understood as being due to the H_2/H reaction providing an extra mechanism by which the liquid can densify. All of these are due to the particular variation of the EOS across this dissociative (or pseudotransition) region. As shown in Fig. 2, the 2000 K isotherm has two intersections with the 1500 K curve (other isotherms are similar). This is a common feature for all transitions or crossovers that induce a *softening* in the compression curve, but at the same time it has a *negative* slope in the phase boundary on the *P-T* space. It should be noted, however, that this is *not* a common feature for all first-order
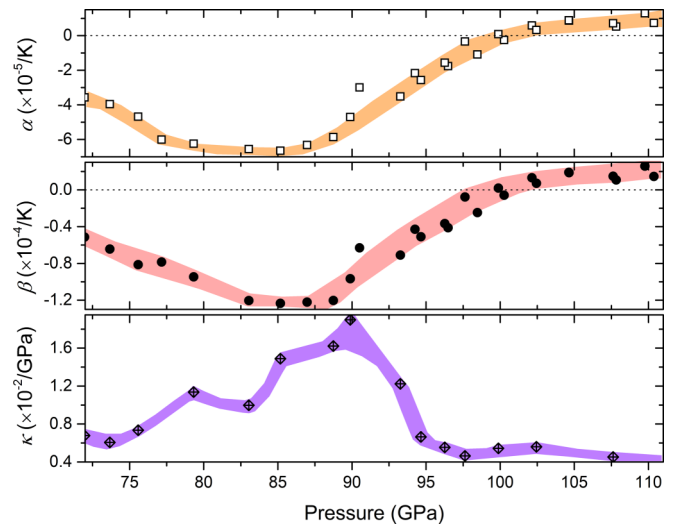

FIG. 3. Estimated thermal expansivity $\alpha = \frac{1}{V}(\frac{\Delta V}{\Delta T})_P$, pressure coefficient $\beta = \frac{1}{P}(\frac{\Delta P}{\Delta T})_V$, and compressibility $\kappa = \frac{-1}{V}(\frac{\Delta V}{\Delta P})_T$ at 2000 K by using the PBE isothermal data. Note the striking *negative* thermal expansivity and pressure coefficient, as well as the anomalously *peaked* compressibility across the dissociation region, indicative of a continuous pseudotransition crossover above the critical point rather than a thermodynamic phase transition. Solid lines are guides to the eye.

transitions that terminate at a critical point, as well as the corresponding supercritical behavior.

This intriguing behavior is similar to a *pseudotransition* in nonstoichiometric compounds, which is inherently continuous, whereas a rapid crossover of the free energy leads to a sharp abnormal variation in the thermodynamics [63,64]. In fact, dimer dissociation at the dilute limit has the same mechanism of pseudotransition [50]. On the other hand, our results showed that these anomalies occur in a broad thermodynamic region both below and beyond the critical point of dense liquid hydrogen. This is a general feature for a dissociative transition of dense molecular liquid that has a negative slope of phase boundary, and it is highly relevant to the interior condition of Jupiter and Saturn, thus it could have a profound impact on the magnetohydrodynamics modeling of convective flows in these planets.

B. Critical point of the LLT

As demonstrated in Fig. 2, the 1000 K isotherm displays a sharp jump and hysteresis at the LLT (a similar result also holds for vdW-DF [50]). This strong signature of a first-order transition unequivocally proves that $T_c \geqslant 1000$ K. At temperatures higher than 1500 K, however, the hysteresis vanishes, and the identification of the nature of the transition requires examining higher derivatives of the free energy, such as heat capacity. Previous claims for the first-order transition (and thus to determine T_c) were based only on a sharp change (or kink) in the isotherms via visual judgment [27,35,44–46]. Unfortunately, identifying a "volume collapse" or kink on a *P-V* curve based on measurements or calculations carried out at discrete volumes is insufficient to validate it as a first-order transition [63,64]. For example, it is hard to tell whether the erratic variation in the 2500 K isotherm (see the
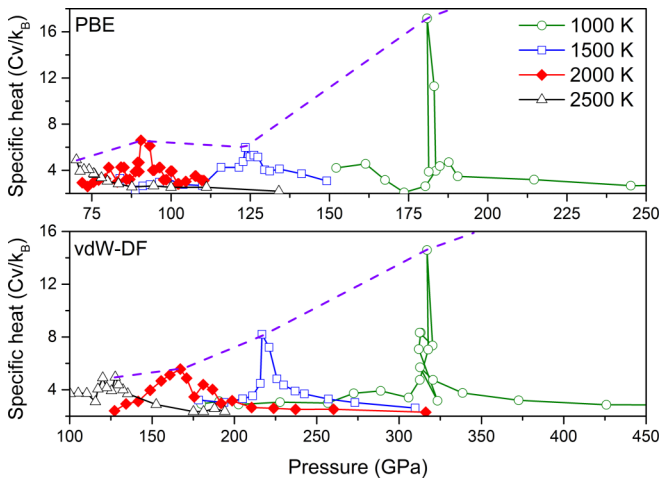
FIG. 4. Specific heat extracted from thermal fluctuations in AIMD simulations at given temperatures calculated with PBE and vdW-DF, respectively. Dashed lines that connect peaks are guides to the eye.

arrow in Fig. 2) is a kink or not. The conclusion depends sensitively on the interval between the discrete data, as well as on the numerical accuracy of pressure measurement. This ambiguity could be one of the reasons for the scattering in the reported T_c estimated using EOS kinks. If we apply the same criterion as used previously, our AIMD data would also give an unphysical T_c higher than 2500 K.

Another method that was used previously to identify the LLT and to locate T_c is the relative variation of RDF [46,47]. The drawback of this approach is that it implicitly assumes that the H_3 cluster is a well-defined stable species. As will be seen below, this is not the case in dissociating hydrogen where the RDF evolves continuously with pressure. Therefore, the method to trace the relative variation of the RDF difference between its first peak and the first valley becomes an arbitrary criterion, since one can instead choose the second peak and the third valley, or any point along the radial distance, as the reference points for the transition. A convincing signature of a first-order transition is *hysteresis*, which was not considered in Refs. [46,47]. Such hysteresis—two densities observed at the same pressure—can be seen in the 1000 K isotherm in Fig. 2.

To locate T_c more reliably, we also employ a different method. It is well known that when approaching a phase transition, thermodynamic fluctuations become large, even being divergent in the case of a first-order transition and closing to the critical point. In a practical AIMD simulation, due to the finite size of the employed supercell, one cannot get a true divergence. However, the fluctuation magnitude could become exceptionally large, so that its variation is sensitive enough to pin down T_c precisely.

According to the fluctuation-dissipation theorem, fluctuations in energy give the specific heat. Such calculated specific heat is plotted in Fig. 4. It shows that at 1000 K the transition is sharp and narrow, being consistent with a first-order transition that approaches the CP. However, it becomes broad and smooth when above 1500 K, illustrating both the width of the crossover region and the position of the Widom line in the supercritical region. The divergence disappears

somewhere between 1000 and 1500 K for both PBE and vdW-DF (with the former being more distinct while the latter is more progressive). This provides unequivocal evidence that a critical point exists for the low-temperature LLT, and T_c should be in this range. This value, ~1250 K, is in good agreement with recent CEIMC assessment [35] and the latest NIF dynamic experiment that observed a sharp transition when below 1080 K but did not resolve a reflectivity jump when beyond 1450 K [51]. As mentioned above, the actual dissociation should be bracketed by the results of PBE and vdW-DF. Figure 4 therefore refutes any theoretical T_c higher than 1500 K [46,47]. It is worth mentioning that our data are also in good agreement with previous PBE results of [45], which revealed a density jump below 1500 K that is driven by an abrupt dissociation with a jump in electrical conductivity, showing the characteristic of a nonmetal-to-metal transition along with dissociation of H_2 molecules. This conclusion marks a *consensus* on T_c between DFT and QMC, as well as between the theory and dynamic compression experiment.

It should be mentioned that because the critical point is close to the melting curve, one might worry about the possible interference of the results from the metastable crystalline-like structures. We carefully checked the simulations of 1000 K, and we did not find any signature of crystalline-like patterns. It should also be pointed out that using the similar DFT setting, we obtained a melting curve in good agreement with other simulations and experimental data [3,20]. Our estimated critical temperature here is ~600 K higher than the melting curve.

C. Possibility of the H_3^+ cluster

In addition to H_2 dimers, larger H-clusters have frequently been predicted as important components in compressed H-rich compounds [5–7] and ultradense solid hydrogen [3]. One of the most common is the H_3 unit. Reference [47] employed a geometric feature in the RDF corresponding to H_3^+ as a criterion to locate T_c. This treatment implicitly assumes that H_3^+ is more important than any other clusters, and it should be a stable chemical species (otherwise one cannot define a new "phase" if the characteristic feature is short-lived, and all related thermodynamics thus must be continuous). Statistical analysis of the CEIMC data suggested that H_3 might not be as stable as previously assumed [49]. Its lifetime, however, has never been explicitly calculated, nor its valence state.

Using AIMD simulations, we obtained the lifetime of individual H_3 clusters, as well as their concentration with temperature and pressure across the dissociation region. The result shows that the lifetime of H_3 units is actually very short (at a level of several fs) [50]. They are too unstable to be regarded as a chemical species. Objects identified as H_3 based on distance criteria [47] are typically transient encounters between H_2 and H, such as scattering, or intermediate states of reactions where one proton displaces another in the dimer. This supports the CEIMC assessment [49]. Furthermore, our Bader charge analysis shows that H_3 is not positively charged with a fixed valence state of +1, as usually expected. Instead, it is on average *neutral*, with a charge state fluctuating frequently between $\pm\delta$ (with $\delta \ll 1$), depending on its rapidly evolving geometry [50]. These observations indicate that the assignment of protons to the big but short-lived clusters is

arbitrary, and might dismiss any evaluation of T_c with reference to H_3^+ ions as in Ref. [47]. These transient clusters do present and manifest in RDF, which, however, is not enough to unambiguously identify a *thermodynamic phase transition* (i.e., a sharp change in this short-lived quantity cannot generally generate a macroscopic discontinuity in the thermodynamic limit).

In addition to H_3, we also observed other larger clusters. All of them have a very short lifetime, and with strong fluctuations in their charge state or polarization [50]. This illustrates that the dissociation is not via a two-step mechanism as proposed in Ref. [47]. Rather, it comprises *multiple* transient and micro consecutive steps of $H_2 \rightarrow H_3 \rightarrow H_n \rightarrow \cdots \rightarrow H$. It also suggests that the complex H-clusters observed in H-rich compounds should originate from a mechanism of heavy elements acting as electron donors or acceptors to balance the charge distribution, which stabilizes certain types of H-clusters within the multiple steps of the dissociation process. It should be noted that the charge fluctuation or sloshing in H-clusters might lead to novel optical properties. For example, it will activate and enhance the otherwise prohibited infrared/Raman modes, and give rise to a strong *noisy optical background* in the dissociating layer of liquid H in Jovian planets.

D. Proton transportation

The sharp first-order LLT in dense hydrogen is associated with discontinuities in transport properties. It was shown that electric conductivity [39] and optical reflectivity [51] jump there, presumably due to metallization. It is thus natural to expect that the transport of protons should also be discontinuous in the vicinity of dissociation.

The AIMD-calculated viscosity based on proton diffusivity using the Stokes-Einstein relationship is shown in Fig. 5. Its variation is quite atypical. With increased pressure, viscosity usually increases, accompanying a reduction in particle mobility. Nonetheless, here we observed a drastic reduction in viscosity with increased pressure when crossing the dissociation region along the isotherms (this effect is equivalent to an enhancement in proton mobility), which saturates to the atomic value after full dissociation [50]. This abnormal decrease in viscosity can be understood by recognizing that lighter, smaller, dissociated H-atoms migrate faster than H_2 molecules. The pressure at which the shift in viscosity occurs depends on the functional, but if viscosity is plotted against a fraction of stable H_2 dimers, the results are independent of the functional.

At the same time, we did not observe any discontinuity or kink in the self-diffusivity of hydrogen at or near $\rho_{H_2} = 0.5$ [50]. This is also different from the usual expectation, showing that the proton mobility is insensitive to the sharp first-order LLT. Overall, our calculation reveals that the proton diffusivity depends more sensitively on the fraction of H rather than H_2, and the rapid increase in proton diffusivity when $\rho_{H_2} \rightarrow 0$ [50] can be understood via a percolation mechanism [65,66].

E. Pseudotransition model

Because of the importance of H_2-dissociation even far beyond T_c as shown above [31,34], it is necessary to derive a

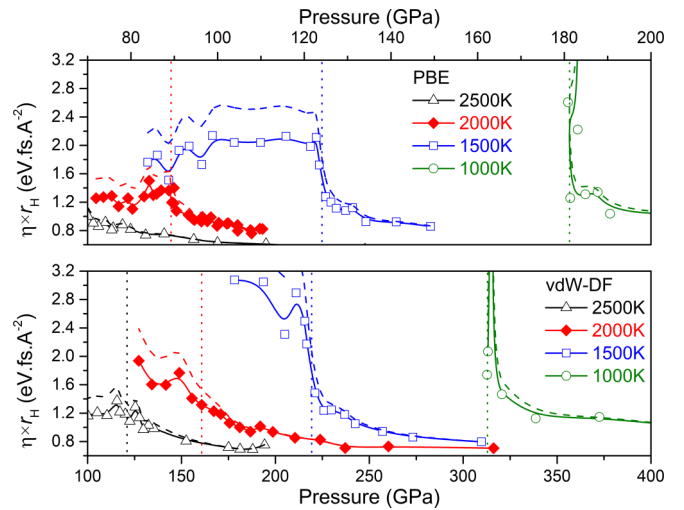FIG. 5. Variation of the viscosity η (with respect to atomic hydrogen radius r_H) of warm dense liquid hydrogen with pressure across the dissociation region calculated from diffusivity using the Stokes-Einstein relationship, using both PBE and vdW-DF, respectively. The vertical dotted lines indicate the position where half of H_2 have been dissociated. The solid(dashed) lines are guides to the eye only, and correspond to the case with a radius ratio of 2(1.6) between H_2 and H particles, respectively.

thermodynamic model to describe this broad and smooth supercritical crossover (including the accompanying anomalies), which is mainly governed by *local* energetics, rather than by collective correlations. It is surprising that the variation of the dissociation width with pressure and temperature qualitatively matches a scenario of the pseudotransition model (PTM) [63,64], which initially was proposed as a thermodynamic crossover in nonstoichiometric compounds that is continuous *a priori*, but which at low enough temperatures can generate sharp kinks in some physical properties, resembling a typical first-order transition [63].

In the case of H_2-dissociation, if we ignore all *local* atomic environment effects, the reaction $H_2 \rightleftharpoons 2H$ can be viewed at the zero-order approximation (i.e., the dilute approximation) as an equilibration in a two-energy level system. The principles of statistical mechanics then give a dimer fraction of $\rho_{H_2} = [\exp(\frac{-\Delta E}{k_B T}) + 1]^{-1}$, which is identical to the result of a PTM [50]. Here ΔE is the binding free energy of H_2 dimers that is a function of pressure and temperature in general, and it can be approximated as $\Delta E(P, T) = a - bP - cT - dTP$. The temperature dependence mainly comes from the contribution of excess entropy before and after the dissociation (i.e., of the 2H against H_2). The pressure dependence comes from bond weakening, from several eV at low pressure approaching zero at about the dissociation pressure.

This PTM captures the main characteristics of the dissociation, as shown in the inset of Fig. 6(a). Reasonable parametrization [50] gives a progressive crossover above 1250 K, but it converges to a sharp LLT when below 1000 K. This AIMD-calculated change of the dissociative transition nature is understandable, since at low temperature and high density the orientation correlation among H_2 dimers is strong, whereas it becomes much weaker at higher temperatures and
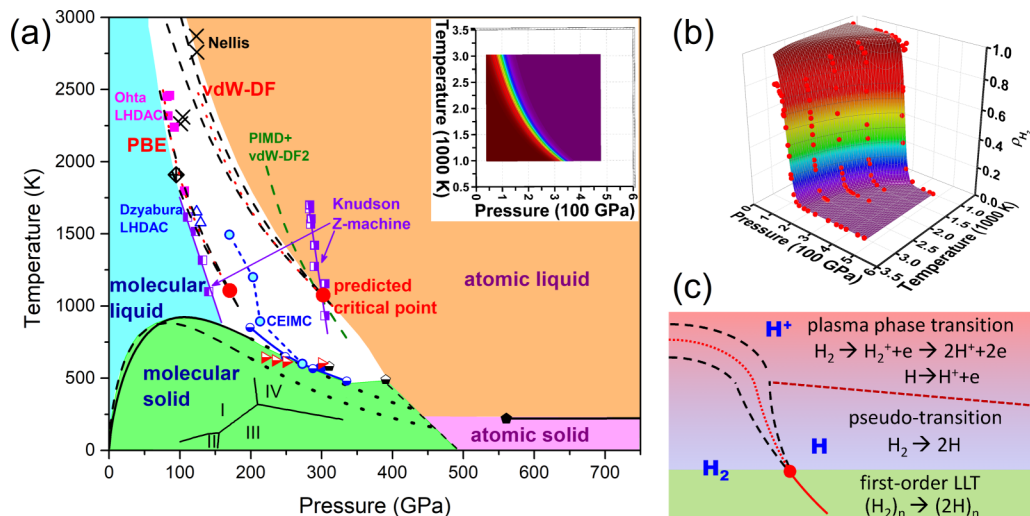
FIG. 6. (a) Phase diagram of warm dense hydrogen around the dissociation region, with PBE and vdW-DF results bracketing the true dissociative transition boundary. The bold black dashed lines represent the 3/7 lines of the dissociation crossover, while the red dotted lines indicate the extension of the first-order LLT boundaries (i.e., the Widom line), with the estimated CP denoted by the red solid circle points, as predicted by PBE and vdW-DF, respectively. The inset shows the dissociation region predicted by vdW-DF fitting to a PTM. The half-filled triangles are the melting points reported by Zha [18]. Note that at the high-temperature limit, both PBE and vdW-DF converge toward the same dissociation curve. The VMC-MD data of Mazzola *et al.* [69] are not included here due to their poor quality of convergence. Other data: CEIMC, Pierleoni [35]; PIMD + vdW-DF2, Morales [54]; half-filled circles, Belonoshko [19]; filled and half-filled pentagons, Geng [3,20]; half-filled squares, Knudson [27]; open triangles, Dzyabura [37]; filled squares, Ohta [38]; crosses, Nellis [70]. (b) H_2 dimer fraction predicted by a PTM compared to the *ab initio* values. (c) A schematic of the three regions of the liquid-H phase diagram, labeled by the dominant species H_2, H, and H^+, and indicating the first-order LLT below T_c and the crossover transitions (including pseudotransition and PPT) elsewhere.

lower densities [67,68]. The vanishing of hysteresis in the high-temperature dissociation region also supports this argument. A schematic representation of this multifaceted scenario is provided in Fig. 6(c).

Figure 6(a) plots the phase diagram of warm dense hydrogen near dissociation. Relevant experimental data available so far are also shown. Zha's melting data [18] constrained the dissociation region from below, and they are in good agreement with Geng [3,20] and Belonoshko's [19] theoretical estimation at about 300 GPa. Our dissociation line calculated with PBE is in remarkable agreement with the laser heating diamond anvil cell (DAC) results [36–38]. This is probably due to an error cancellation with too weakly bonded PBE molecules compensating for the absent zero-point energy (ZPE) weakening; moreover, the DAC data are still under debate [51]. The CEIMC estimate [35], which includes both ZPE and QMC exchange-correlation effects at the expense of describing the two "liquids" with a total of 27 molecules, lies midway between our PBE and vdW-DF results, and is in good agreement with the laser-shock measurement of the reflectivity [51]. The latter data are not shown here for the sake of clarity. To show the width of the crossover region, the AIMD-calculated 3/7 lines (that correspond to an H_2 dimer fraction of 30% and 70%, respectively) are also plotted. These lines, together with the PTM results, narrow the uncertainty range of T_c for the first-order LLT further down to between 1250 and 1000 K, far below the previous DFT estimate of ~2000 K (the crossed rhombus point in Fig. 6) [27,44,45]. This new DFT estimate, however, is in good agreement with the latest experimental [51] and CEIMC [35] data. Above this point, the dissociative transition has a *finite width* on the *P-T*

plane, and the boundary cannot be characterized by a single line any more.

IV. FURTHER DISCUSSION

The assignment of the low-temperature dissociation and metallization transition in dense liquid hydrogen as a plasma phase transition has its historical reasons, but our work shows this to be untenable. The electron localization function (Fig. 7) demonstrates that even in the metallic state, the electrons are strongly associated with the ions, whereas
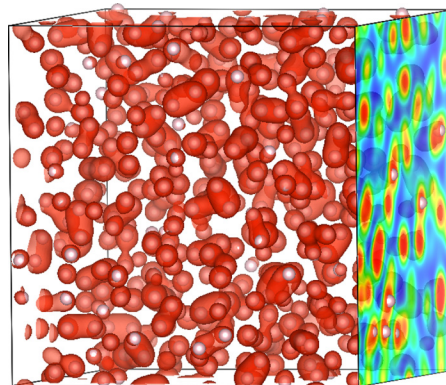

FIG. 7. Electron localization function isosurface (with ELF = 0.92, in red) for liquid H_2 within the dissociation region at 138.5 GPa and 1500 K (with an atomic volume of 1.9512 Å^3/H) calculated by PBE. An ELF plane is also included [ELF going from 0 (blue) to 1 (red)].

the plasma transition should denote the ionization process of $H_2 \rightarrow H_2^+ + e \rightarrow 2H^+ + 2e$. The nature of this latter ultrahigh-temperature transition, however, is completely different from what occurs at just above the critical point. As shown in Fig. 7, the electrons are still localized around the atomic nucleus or covalent bond centers at these conditions. The dissociation and metallization processes in both the subcritical and supercritical regions are via orbital overlapping and the subsequent (partial) electron delocalization, rather than ionization. This observation is corroborated by charge analysis, where some atomic hydrogen is even negatively charged [50], strong evidence that it is not an ionization process. For this reason, we suggest reserving the name PPT for the transition at ultrahigh temperature that is obtained by the kinetic ionization process and extends to ultrahigh solar conditions; between PPT and the critical point (i.e., the supercritical region), the transition is a continuous crossover, characterized by orbital overlapping and electron delocalization, but with very weak intermolecular correlations, which we would like to call a *pseudotransition* to emphasize its unique dimer-dissociative characteristics that are not shared by normal supercritical crossover; below the critical point, the transition is also driven by electron wave-function overlap and delocalization, but now with strong intermolecular correlations and the resultant discontinuities in density and other physical quantities, and this regime in the subcritical region is a *first-order LLT*. These *three* distinct regimes of the dissociative liquid-liquid transition are schematically shown in Fig. 6(c). It provides a comprehensive scenario for the temperature-pressure-driven metallization and ionization in warm dense liquid hydrogen.

It should be pointed out that the dimer fraction in H_2 dissociation is the proper order parameter for the transition, which correctly reproduces the prohibited region in the order parameter space as required by the Landau theory of the phase transition [50]. Most previous studies on this topic tried to understand the transition in the density space. Unfortunately, the density difference between the atomic and molecular liquid phases is *not* a proper order parameter for this dissociative transition. This, together with the pseudotransition nature of the dissociation, which could also lead to a continuous but "sharp" variation in physical quantities, contributed to the controversial nature and scattered CP location of this transition as reported in the literature. The finite-size effect complicates this further [50].

There is a general consensus on the coincidence of metallization and dissociation in dense liquid hydrogen. By using the dimer fraction as an order parameter, we showed in Fig. 6(b) that beyond the thermodynamic critical point of ∼1250 K, the dissociative transition has a *finite* width on the *P-T* plane, so it *cannot* be a first-order transition. However, one might argue that the first-order transition could be different from the dissociative transition, thus it can coexist with the latter simultaneously. Such a hypothesis—that there is another first-order transition existing *within* the broad dissociative region beyond the critical point, as shown by the dotted red line in Fig. 6(c)—is intriguing. The band gap appears to drop continuously to zero, which does not imply any first-order transition. The region defined by an electron density isosurface undergoes a percolation transition, but at different

densities depending on its chosen value. We did not find any other order parameter with discontinuity in our AIMD simulations above the critical point. This can be understood by recognizing that the collective motion in any first-order transition must come from some correlations. As we showed above, intermolecular correlation is very weak in liquid hydrogen [50]. The main contribution is the angular orientation arising from the compression effect. At low pressure, the intermolecular distance becomes large enough so that it loses all orientation correlations. This can be seen clearly in Fig. 6, in which the CP of PBE is at such a low pressure, whose low-temperature region is occupied by phase I, that it does not have any dimer orientation correlations. That is to say, in the liquid state at high temperature of the same density or below, it is unlikely that there will still be interparticle correlations (other than the dissociation itself) to cause a first-order transition.

The results we revealed above might have an impact on the modeling of the convective flow across the H_2/H layer and the dynamo of cold giant gas planets [34]. The low T_c of both our DFT and CEIMC implies the irrelevance of the first-order LLT to the interior of Jupiter and Saturn. Even if this transition occurs in a very cold gas planet, our calculation predicts that the H_2/H interface is volatile, and H_2 and H are *miscible*. Its direct influence on the convective flow is thus much less significant than previously estimated. On the other hand, our results also suggested that strong thermodynamic anomalies (e.g., negative thermal expansion) extend far above T_c. This *P-T* condition is directly relevant to the interior of Jupiter and Saturn. For example, along Jupiter's adiabat, DFT calculations revealed an anomalous peak in heat capacity and a dip in thermal expansivity that occur exactly in the dissociation region [71]. This is qualitatively in line with our results as presented in Figs. 3 and 4 even though the composition is different, the temperature is much higher, and the pressure is lower. The hydrogen diffusivity along Jupiter's adiabat as reported in [71] also jumps when crossing the dissociation region, and the numerical value near the dissociation is comparable to our data. This confirms that anomalies associated with dissociation can extend very far beyond the critical point. This striking "wide-range" influence arises from the unique behavior of molecular dissociation (i.e., the pseudotransition mechanism), and it cannot be accounted for by *normal* supercritical behavior. The observed thermodynamic anomalies, together with the predicted anomalous drop of viscosity across the dissociation, contribute to the thermal instability of convection cells and the internal dynamics of cold giant gas planets. For example, the large-scale convection cell in gas planets could be cut by this anomalous layer into two parts, changing the convection flow cycle from a usual "O" shape into an "8" shape, and resulting in an advection layer in between [50].

V. CONCLUSION

In summary, the complex nature of a liquid-liquid transition in hydrogen was investigated with AIMD simulations. We find a first-order thermodynamic transition line that terminates at a critical point. Above the critical point, the molecular-atomic transformation causes anomalies in the viscosity and thermal expansivity.

This broad and smooth supercritical crossover region, and the accompanying anomalies, can be described by a pseudo-transition model. Going from low pressure to high pressure, compression enhances interparticle interactions, weakens the covalent bonds, and modifies the dimer binding energy. This lowers the corresponding dissociation temperature from ionization energy to much lower temperature. Compression also puts strong constraints on molecular rotations, but it subsequently enhances *local* angular orientation correlations, leading to large but transient H-clusters during dissociation. At low enough temperature, the dissociative transition eventually develops into a first-order LLT when below ~1250 K. Unlike typical first-order transitions, the H_2/H two-phase coexistence interface of this LLT is unstable, and the parent-daughter phases are *miscible*, which is a general feature for such a dissociative transition with a large negative slope of dT/dP along the boundary. This density-driven LLT is comparable to the solid phase I-III–metal transition, while the miscibility of H/H_2 species is reminiscent of the atomic-molecular solid phase IV. Finally, other facets of the transition as discovered in this work, e.g., the thermodynamic anomalies due to pseudotransition and the counterintuitive variation of the proton diffusivity and viscosity in the vicinity of dissociation, could have a significant impact on the modeling of the interior of cold Jovian planets.

[1] J. M. McMahon, M. A. Morales, C. Pierleoni, and D. M. Ceperley, The properties of hydrogen and helium under extreme conditions, Rev. Mod. Phys. **84**, 1607 (2012).

[2] H. Y. Geng, Q. Wu, and Y. Sun, Prediction of a mobile solid state in dense hydrogen under high pressures, J. Phys. Chem. Lett. **8**, 223 (2017).

[3] H. Y. Geng and Q. Wu, Predicted reentrant melting of dense hydrogen at ultra-high pressures, Sci. Rep. **6**, 36745 (2016).

[4] H. Wang, X. Li, G. Gao, Y. Li, and Y. Ma, Hydrogen-rich superconductors at high pressures, WIREs Comput. Mol. Sci. **8**, e1330 (2018).

[5] D. Duan, Y. Liu, Y. Ma, Z. Shao, B. Liu, and T. Cui, Structure and superconductivity of hydrides at high pressures, Natl. Sci. Rev. **4**, 121 (2017).

[6] E. Zurek, Hydrides of the alkali metals and alkaline earth metals under pressure, Commun. Inorg. Chem. **37**, 78 (2017).

[7] Y. Chen, H. Y. Geng, X. Yan, Y. Sun, Q. Wu, and X. Chen, Prediction of stable ground-state lithium polyhydrides under high pressures, Inorg. Chem. **56**, 3867 (2017).

[8] H. K. Mao and R. J. Hemley, Ultrahigh-pressure transitions in solid hydrogen, Rev. Mod. Phys. **66**, 671 (1994).

[9] R. T. Howie, P. Dalladay-Simpson, and E. Gregoryanz, Raman spectroscopy of hot hydrogen above 200 GPa, Nat. Mater. **14**, 495 (2015).

[10] P. Dalladay-Simpson, R. T. Howie, and E. Gregoryanz, Evidence for a new phase of dense hydrogen above 325 gigapascals, Nature (London) **529**, 63 (2016).

[11] R. P. Dias, O. Noked, and I. F. Silvera, New Phases and Dissociation- Recombination of Hydrogen Deuteride to 3.4 Mbar, Phys. Rev. Lett. **116**, 145501 (2016).

[12] M. I. Eremets, I. A. Troyan, and A. P. Drozdov, Low temperature phase diagram of hydrogen at pressures up to 380 GPa. A possible metallic phase at 360 GPa and 200 K, arXiv:1601.04479.

[13] C. J. Pickard and R. J. Needs, Structure of phase III of solid hydrogen, Nat. Phys. **3**, 473 (2007).

[14] I. B. Magdau, M. Marques, B. Borgulya, and G. J. Ackland, Simple thermodynamic model for the hydrogen phase diagram, Phys. Rev. B **95**, 094107 (2017).

[15] I. B. Magdau and G. J. Ackland, Identification of high-pressure phases III and IV in hydrogen: Simulating Raman spectra using molecular dynamics, Phys. Rev. B **87**, 174110 (2013).

[16] S. A. Bonev, E. Schwegler, T. Ogitsu, and G. Galli, A quantum fluid of metallic hydrogen suggested by first-principles calculations, Nature (London) **431**, 669 (2004).

[17] M. I. Eremets and I. A. Trojan, Evidence of maximum in the melting curve of hydrogen at megabar pressures, JETP Lett. **89**, 174 (2009).

[18] C. Zha, H. Liu, J. S. Tse, and R. J. Hemley, Melting and High P-T Transitions of Hydrogen up to 300 GPa, Phys. Rev. Lett. **119**, 075302 (2017).

[19] A. B. Belonoshko, M. Ramzan, H. K. Mao, and R. Ahuja, Atomic diffusion in solid molecular hydrogen, Sci. Rep. **3**, 2340 (2013).

[20] H. Y. Geng, R. Hoffmann, and Q. Wu, Lattice stability and high-pressure melting mechanism of dense hydrogen up to 1.5 TPa, Phys. Rev. B **92**, 104103 (2015).

[21] J. Chen, X. Z. Li, Q. Zhang, M. I. J. Probert, C. J. Pickard, R. J. Needs, A. Michaelides, and E. Wang, Quantum simulation of low-temperature metallic liquid hydrogen, Nat. Commun. **4**, 2064 (2013).

[22] R. P. Dias and I. F. Silvera, Observation of the Wigner-Huntington transition to metallic hydrogen, Science **355**, 715 (2017).

[23] H. Y. Geng, Public debate on metallic hydrogen to boost high pressure research, Matter Rad. Extremes **2**, 275 (2017).

[24] N. W. Ashcroft, The hydrogen liquids, J. Phys.: Condens. Matter **12**, A129 (2000).

[25] E. Babaev, A. Sudbø, and N. W. Ashcroft, A superconductor to superfluid phase transition in liquid metallic hydrogen, Nature (London) **431**, 666 (2004).

[26] E. Babaev, A. Sudbø, and N. W. Ashcroft, Observability of a Projected New State of Matter: A Metallic Superfluid, Phys. Rev. Lett. **95**, 105301 (2005).

[27] M. D. Knudson, M. P. Desjarlais, A. Becker, R. W. Lemke, K. R. Cochrane, M. E. Savage, D. E. Bliss, T. R. Mattsson, and R. Redmer, Direct observation of an abrupt insulator-to-metal transition in dense liquid deuterium, Science **348**, 1455 (2015).

[28] I. I. Naumov, R. J. Hemley, R. Hoffmann, and N. W. Ashcroft, Chemical bonding in hydrogen and lithium under pressure, J. Chem. Phys. **143**, 064702 (2015).

[29] H. Y. Geng, H. X. Song, J. F. Li, and Q. Wu, High-pressure behavior of dense hydrogen up to 3.5 TPa from density functional theory calculations, J. Appl. Phys. **111**, 063510 (2012).

[30] V. Labet, R. Hoffmann, and N. W. Ashcroft, A fresh look at dense hydrogen under pressure. III. Two competing effects and the resulting intra-molecular H-H separation in solid hydrogen under pressure, J. Chem. Phys. **136**, 074503 (2012); A fresh look at dense hydrogen under pressure. IV. Two structural models on the road from paired to monatomic hydrogen, via a possible non-crystalline phase, **136**, 074504 (2012).

[31] H. M. Van Horn, Dense astrophysical plasmas, Science **252**, 384 (1991).

[32] D. Saumon and G. Chabrier, Fluid Hydrogen at High Density: The Plasma Phase Transition, Phys. Rev. Lett. **62**, 2397 (1989).

[33] D. Saumon and G. Chabrier, Fluid hydrogen at high density: Pressure ionization, Phys. Rev. A **46**, 2084 (1992).

[34] W. J. Nellis, S. T. Weir, and A. C. Mitchell, Metallization and electrical conductivity of hydrogen in Jupiter, Science **273**, 936 (1996).

[35] C. Pierleoni, M. A. Morales, G. Rillo, M. Holzmann, and D. M. Ceperley, Liquid-liquid phase transition in hydrogen by coupled electron-ion Monte Carlo simulations, Proc. Natl. Acad. Sci. (USA) **113**, 4953 (2016).

[36] M. Zaghoo, A. Salamat, and I. F. Silvera, Evidence of a first-order phase transition to metallic hydrogen, Phys. Rev. B **93**, 155128 (2016).

[37] V. Dzyabura, M. Zaghoo, and I. F. Silvera, Evidence of a liquid-liquid phase transition in hot dense hydrogen, Proc. Natl. Acad. Sci. (USA) **110**, 8040 (2013).

[38] K. Ohta, K. Ichimaru, M. Einaga, S. Kawaguchi, K. Shimizu, T. Matsuoka, N. Hirao, and Y. Ohishi, Phase boundary of hot dense fluid hydrogen, Sci. Rep. **5**, 16560 (2015).

[39] B. Holst, M. French, and R. Redmer, Electronic transport coefficients from *ab initio* simulations and application to dense liquid hydrogen, Phys. Rev. B **83**, 235120 (2011).

[40] W. R. Magro, D. M. Ceperley, C. Pierleoni, and B. Bernu, Molecular Dissociation in Hot, Dense Hydrogen, Phys. Rev. Lett. **76**, 1240 (1996).

[41] K. T. Delaney, C. Pierleoni, and D. M. Ceperley, Quantum Monte Carlo Simulation of the High-Pressure Molecular-Atomic Crossover in Fluid Hydrogen, Phys. Rev. Lett. **97**, 235702 (2006).

[42] D. Saumon and G. Chabrier, Fluid hydrogen at high density: Pressure dissociation, Phys. Rev. A **44**, 5122 (1991).

[43] B. Holst, R. Redmer, and M. P. Desjarlais, Thermophysical properties of warm dense hydrogen using quantum molecular dynamics simulations, Phys. Rev. B **77**, 184201 (2008).

[44] M. A. Morales, C. Pierleoni, E. Schwegler, and D. M. Ceperley, Evidence for a first-order liquid-liquid transition in high-pressure hydrogen from *ab initio* simulations, Proc. Natl. Acad. Sci. (USA) **107**, 12799 (2010).

[45] W. Lorenzen, B. Holst, and R. Redmer, First-order liquid-liquid phase transition in dense hydrogen, Phys. Rev. B **82**, 195107 (2010).

[46] G. Mazzola, R. Helled, and S. Sorella, Phase Diagram of Hydrogen and a Hydrogen-Helium Mixture at Planetary Conditions by Quantum Monte Carlo Simulations, Phys. Rev. Lett. **120**, 025701 (2018).

[47] G. Norman and I. Saitov, Critical point and mechanism of the fluid-fluid phase transition in warm dense hydrogen, Dokl. Phys. **62**, 294 (2017).

[48] C. Tian, F. Liu, H. Yuan, H. Chen, and A. Kuan, First-order liquid-liquid phase transition in compressed hydrogen and critical point, J. Chem. Phys. **150**, 204114 (2019).

[49] C. Pierleoni, M. Holzmann, and D. M. Ceperley, Local structure in dense hydrogen at the liquid-liquid phase transition by coupled electron-ion Monte Carlo, Contrib. Plasma Phys. **58**, 99 (2018).

[50] See Supplemental Material at http://link.aps.org/supplemental/10.1103/PhysRevB.100.134109 for results of the dimer-dimer bond-length distribution (DDLD) calculations, a comparison between PBE and vdW-DF results, the thermodynamic modeling of pseudotransition and phase boundaries, calculated isotherms (EOS), transient clusters and their lifetime and charge state, the angular distribution function of H_3 clusters, mixing of H and H_2 liquid, thermal fluctuation analysis, the isotope effect, finite-size effects, and an assessment of proton self-diffusivity and viscosity.

[51] P. M. Celliers, M. Millot, S. Brygoo, R. S. McWilliams, D. E. Fratanduono, J. R. Rygg, A. F. Goncharov, P. Loubeyre, J. H. Eggert, J. L. Peterson, N. B. Meezan, S. L. Pape, G. W. Collins, R. Jeanloz, and R. J. Hemley, Insulator-metal transition in dense fluid deuterium, Science **361**, 677 (2018).

[52] M. Dion, H. Rydberg, E. Schröder, D. C. Langreth, and B. I. Lundqvist, Van Der Waals Density Functional for General Geometries, Phys. Rev. Lett. **92**, 246401 (2004).

[53] J. Klimeš, D. R. Bowler, and A. Michaelides, Van der Waals density functionals applied to solids, Phys. Rev. B **83**, 195131 (2011).

[54] M. A. Morales, J. M. McMahon, C. Pierleoni, and D. M. Ceperley, Nuclear Quantum Effects and Nonlocal Exchange-Correlation Functionals Applied to Liquid Hydrogen at High Pressure, Phys. Rev. Lett. **110**, 065702 (2013).

[55] M. A. Morales, J. M. McMahon, C. Pierleoni, and D. M. Ceperley, Towards a predictive first-principles description of solid molecular hydrogen with density functional theory, Phys. Rev. B **87**, 184107 (2013).

[56] M. D. Knudson and M. P. Desjarlais, High-Precision Shock Wave Measurements of Deuterium: Evaluation of Exchange-Correlation Functionals at the Molecular-to-Atomic Transition, Phys. Rev. Lett. **118**, 035501 (2017).

[57] S. Azadi and G. J. Ackland, The role of van der Waals and exchange interactions in high-pressure solid hydrogen, Phys. Chem. Chem. Phys. **19**, 21829 (2017).

[58] G. J. Ackland and I. B. Magdau, Appraisal of the realistic accuracy of molecular dynamics of high-pressure hydrogen, Cogent Phys. **2**, 1049477 (2015).

[59] I. B. Magdau and G. J. Ackland, Charge density wave in hydrogen at high pressure, J. Phys.: Conf. Ser. **950**, 042058 (2017).

[60] T. Ogitsu, E. Schwegler, F. Gygi, and G. Galli, Melting of Lithium Hydride under Pressure, Phys. Rev. Lett. **91**, 175502 (2003).

[61] J. R. Morris, C. Z. Wang, K. M. Ho, and C. T. Chan, Melting line of aluminum from simulations of coexisting phases, Phys. Rev. B **49**, 3109 (1994).

[62] I. Iosilevskiy, Non-congruent phase transitions in cosmic matter and in the laboratory, Acta Phys. Pol. B Proc. Suppl. **3**, 589 (2010).

[63] H. Y. Geng, H. X. Song, and Q. Wu, Anomalies in nonstoichiometric uranium dioxide induced by a pseudo phase transition of point defects, Phys. Rev. B **85**, 144111 (2012).

[64] H. Y. Geng, H. X. Song, and Q. Wu, Theoretical assessment on the possibility of constraining point-defect energetics by pseudo phase transition pressures, Phys. Rev. B **87**, 174107 (2013).

[65] T. Lundh, Percolation diffusion, Stoch. Proc. Appl. **95**, 235 (2001).

[66] R. Perriot, B. P. Uberuaga, R. J. Zamora, D. Perez, and A. F. Voter, Evidence for percolation diffusion of cations and reordering in disordered pyrochlore from accelerated molecular dynamics, Nat. Commun. **8**, 618 (2017).

[67] I. Tamblyn and S. Bonev, Structure and Phase Boundaries of Compressed Liquid Hydrogen, Phys. Rev. Lett. **104**, 065702 (2010).

[68] W. Grochala, R. Hoffmann, J. Feng, and N. W. Ashcroft, The chemical imagination at work in very tight places, Angew. Chem. **46**, 3620 (2007).

[69] G. Mazzola and S. Sorella, Distinct Metallization and Atomization Transitions in Dense Liquid Hydrogen, Phys. Rev. Lett. **114**, 105701 (2015).

[70] W. Nellis, S. Weir, and A. Mitchell, Minimum metallic conductivity of fluid hydrogen at 140 GPa (1.4 Mbar), Phys. Rev. B **59**, 3434 (1999).

[71] M. French, A. Becker, W. Lorenzen, N. Nettelmann, M. Bethkenhagen, J. Wicht, and R. Redmer, *Ab initio* simulations for material properties along the Jupiter adiabat, Astrophys. J. Suppl. Series **202**, 5 (2012).